Microscopic mechanisms for photoinduced metastability in amorphous As_2S_3

T. Uchino* and D. C. Clary
Department of Chemistry, University College London, 20 Gordon Street, London, WC1H 0AJ, United Kingdom

S. R. Elliott
Department of Chemistry, University of Cambridge, Lensfield Road, CB2 1EW, Cambridge, United Kingdom
(Received 15 October 2001; revised manuscript received 29 January 2002; published 29 April 2002)

Using clusters of atoms that model the local structure of amorphous As_2S_3 (a-As_2S_3), we here present a model of photoinduced structural changes in a-As_2S_3. We have performed quantum-chemical calculations on the model clusters and have obtained their equilibrium configurations, charge distributions, molecular-orbital structures, and excitation energies. It has been found that there exist at least two types of metastable structural defects. One has a fivefold-coordinated As unit, and the other comprises a fourfold-coordinated As atom and a nonbridging S atom. Each type of defect results from the breaking of an As-S bond and subsequent structural rearrangement. From the calculations of the excitation energies, we suggest that the fivefold As defect is responsible for a parallel redshift of the optical absorption edge upon light exposure, called photodarkening. On the other hand, the fourfold As defect is likely to contribute to the photoinduced midgap absorption below ~2 eV induced by low-temperature light exposure. It has also been demonstrated that the formation of these metastable defects is closely associated with interlayer atomic reconfigurations resulting in homopolar As-As linkages.

DOI: 10.1103/PhysRevB.65.174204 PACS number(s): 71.55.Jv, 78.66.Jg, 73.61.Jc

I. INTRODUCTION

Photoinduced changes in the structure generally occur in materials having structural flexibility or relatively large internal free volume. Another possible factor leading to photoinduced phenomena is strong localization of the photoexcited electron-hole pairs, which may change the valency and/or coordination number of the atoms involved in the charge localization. This localization can thus be envisaged as a charged defect state from the view of the structure. These factors pertaining to photoinduced phenomena are characteristic of amorphous systems, and, therefore, photoinduced structural and chemical changes are observed in glassy materials.[1,2]

Amorphous chalcogenides, in particular, show a number of interesting photoinduced changes not only in the structure,[3–10] but also in the paramagnetic,[11,12] electronic,[13,14] and optical properties,[15,16] which prepared the ground for various electronic switching and memory devices, optical memories, and imaging applications. Thus far, a large number of studies have been carried out to gain a better understanding of metastable photoinduced effects in chalcogenide glasses, and various mechanisms have been proposed to account for their origin.[1,10,17–23] However, no conclusive picture of photoinduced phenomena has yet been given, and the nature of the photoinduced metastability is still a subject of profound discussions.

Recently, quantum-chemical calculations have proved increasingly useful for the study of the structure and properties associated especially with defect centers in amorphous materials.[24–28] In our previous paper,[29] we have employed a quantum-chemical approach to give a theoretical basis for various photoinduced phenomena observed in amorphous As_2S_3 (a-As_2S_3). It is probable that in amorphous solids, electrons and holes excited into the states which extend from the band edges into the gap localize quickly in these band-tail states before recombination takes place.[2] According to this scheme, localization of the charge carriers is a reasonable model of the photoexcited states of the corresponding disordered system. Thus we calculated the equilibrium geometry of the electron- and hole-trapping centers in a-As_2S_3 using clusters of atoms that model the localization of the respective charge carriers. We then investigated how these charged defects relaxed after recombination. As a result of the calculations, we found the following: (1) The model cluster consisting of connected AsS_3 trigonal pyramids is apt to trap an electron, followed by breaking of one of the As-S bonds in AsS_3 units. (2) A metastable fivefold-coordinated As site, having four As-S bonds and one As-As bond, is formed after recombination of the negatively as well as of the positively charged defect. (3) This fivefold-coordinated As center is an unprecedented coordination defect, which exhibits a lower electronic excitation energy than the normal AsS_3 trigonal bipyramidal unit by ~1 eV. We[29] have hence proposed that the photodarkening effect of a-As_2S_3—namely, a shift of the absorption edge to lower energies upon near-band-gap illumination—can be interpreted in terms of a structural conversion from threefold to fivefold coordination of the basic building unit via a photoionization process.

Although the above work is a reasonable first theoretical attempt to explain the complex photoinduced phenomena, the model clusters employed were rather small. These clusters comprised only three As atoms, neglecting the surrounding environments around the defect of interest. Thus larger clusters would be more favorable to convince one that the structural changes are correctly modeled by this procedure. In this paper, we therefore employ clusters of atoms consisting of seven As atoms to model the ground state, as well as metastable configurations of a-As_2S_3. Using these rather

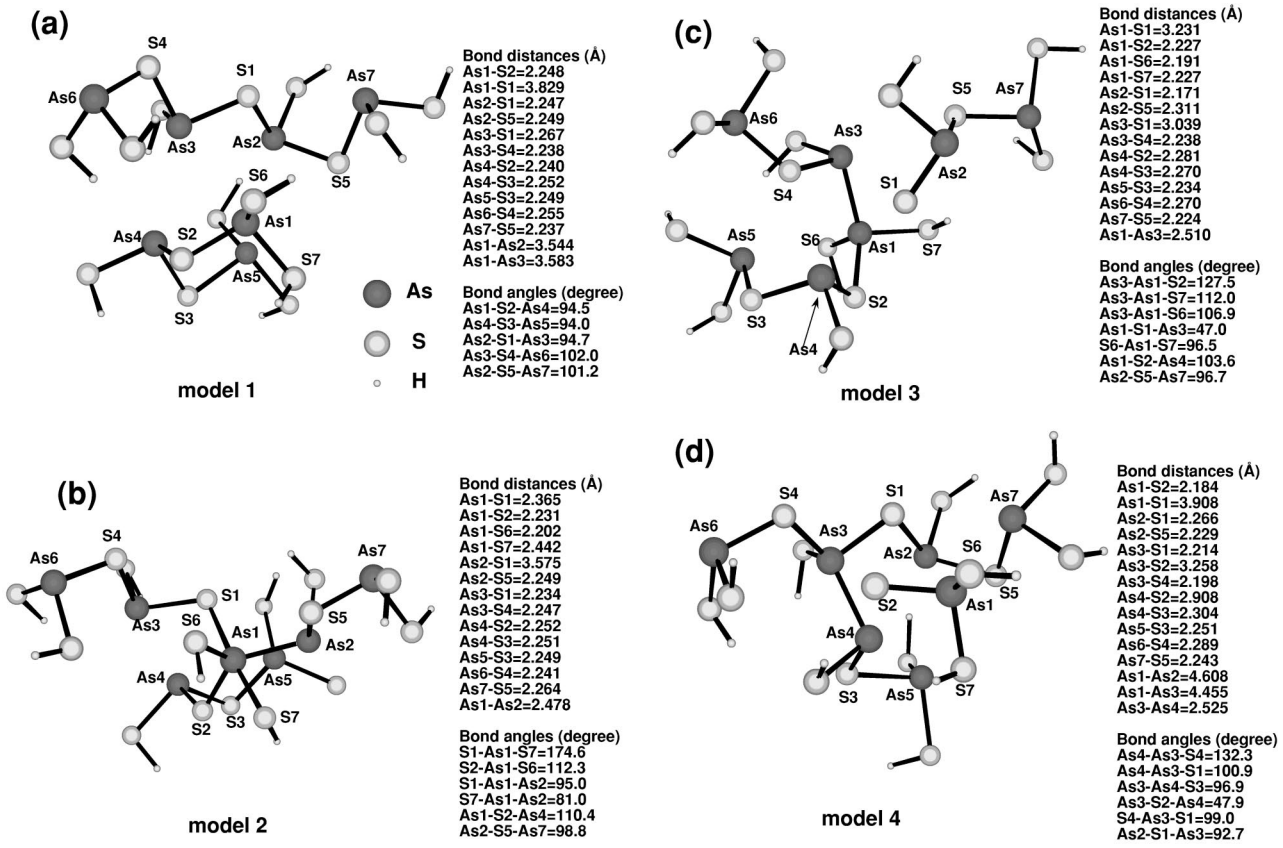

FIG. 1. Optimized geometries of the $As_7S_{16}H_{11}$ cluster calculated at the HF/6-31G(d) level. A ground-state configuration is shown in (a) (model 1). Three metastable configurations derived from the breaking of the As2-S1, As3-S1, and As4-S2 bonds are shown in (b) (model 2), (c) (model 3), and (d) (model 4), respectively. Principal bond distances and bond angles are shown.

large clusters, we investigate local photoinduced structural changes resulting from recombination events of the excited charge carriers. We show that the basic conclusions reached previously are also applicable to the present case. Moreover, the present calculations reveal another metastable coordination defect that exhibits a much lower electronic excitation energy than the fivefold-coordinated As unit.

II. MODELS AND CALCULATIONAL PROCEDURES

We used a cluster of atoms having seven AsS_3 units as a model of the ideally well-annealed network of a-As_2S_3 [model 1: see Fig. 1(a)]. Since it is highly likely that the photoinduced processes involve atomic rearrangements in both interlayer and intralayer configurations, model 1 consists of two subunits having four and three connected AsS_3 units, respectively, that interact with each other through weak nonbonding interactions or van der Waals forces. The outermost S atoms in the cluster were terminated by H atoms. Of course, H termination of clusters is not real, but is employed to suppress the ''surface'' effect arising from the dangling bonds of the outermost atoms. Thus far, such H-terminated models have been tested by a number of researchers, and it has been well recognized that the method of hydrogen saturation is not far from realistic, but is a useful method to eliminate the unsaturated bonds of clusters modeling the local structure of the corresponding amorphous system.[30] The geometry of the cluster was optimized at the Hartree-Fock (HF) level without imposing any structural constraints. All *ab initio* molecular-orbital calculations in this work were performed with the 6-31G(d) basis set[31] using the GAUSSIAN 98 computer program.[32]

As has been pointed out in the Introduction, one possible action of band-gap or sub-band-gap illumination is to weaken and ultimately break bonds, preceded by the localization of the photoexcited charge carriers at the band edges. These trapped charges change the local valency and induce further bond rearrangements after recombination, which eventually results in the observed photostructural changes. In order to simulate such photoinduced bond-breaking and subsequent recombination processes, we intentionally elongated one of the As-S bonds in model 1. The value of elongation (Δr) employed was 1.2 Å since we[29] have found previously that the As-S bond distance increases from ~2.2 to ~3.4 Å upon trapping an electron. Using such deformed configurations as an initial geometry, we then carried out a full geometry optimization at the HF/6-31G(d) level as well. For this purpose, we elongated in model 1 the As2-S1 bond [generating model 2: see Fig. 1(b)], the As3-S1 bond [generating model 3: see Fig. 1(c)], and the As4-S2 bond [generating model 4: see Fig. 1(d)]; it was assumed that the total charge and multiplicity of each cluster was 0 and 1, respectively, as

TABLE I. Average As-S bond distances (in Å) and As-S-As bond angles (in degrees) calculated for the model clusters.

	Model 1	Model 2	Model 3	Model 4
As-S	2.242	2.255	2.242	2.238
As-S-As	97.3	101.9	99.8	101.0

in the case of model 1. Thus the obtained geometries can be regarded as being diamagnetic metastable defects of the random As_2S_3 network.

Atomic charges of the model clusters were obtained from a Mulliken population analysis.[33] Time-dependent density-functional response theory (TD-DFRT) was used for the calculation of electronic excitation energies.[34] It has been demonstrated that the average absolute error of the TD-DFRT is closer to that of the computationally more costly correlated *ab initio* methods such as configuration interaction methods.[34] Since hybrid functionals have been shown to yield more accurate excitation energies than gradient-corrected functionals,[35] we used the Becke 1993 hybrid exchange functional, which includes a mixture of HF and density-functional theory exchange, with the Lee-Yang-Parr correlation energy functional[36] (B3LYP) and the 6-31G(d) basis set augmented by one set of diffuse functions on As and S atoms[32] [6-31+G(d)] to calculate the TD-DFRT excitation energies. These diffuse functions are necessary to describe both valence and Rydberg-type excitations on an equal footing.

III. RESULTS

A. Optimized geometry

Figure 1(a) shows the optimized geometry of model 1 calculated at the HF/6-31G(d) level. The average intramolecular As-S bond distance and As-S-As bond angle calculated for model 1 are listed in Table I. We see from Table I that the calculated As-S bond distance (2.242 Å) is in reasonable agreement with the average As-S bond distance observed for annealed a-As_2S_3 films (2.280 Å).[8] It should be noted that the observed As-S-As bond angle[8] (~100°) is also quantitatively reproduced by the present cluster calculation (97.3°). The smaller cluster reported in a previous paper[29] gave a larger value (118.9°) for the As-S-As bond angle than the observed one (~100°). Thus we consider that the present larger cluster will more reasonably represent possible strains and weak van der Waals forces between the As-S-As linkages in actual amorphous solids.

We next turn to the optimized configurations of model 2 [see Fig. 1(b)], in which the As2-S1 bond of model 1 was intentionally elongated. The total energy of model 2 was found to be higher than that of model 1 by 2.05 eV, indicating that the defect configuration in model 2 is indeed a metastable structure. The resultant As2-S1 interatomic distance in model 2 was 3.575 Å, indicating that the original As2-S1 covalent bond in model 1 was broken as a result of the present bond-elongation process. In model 2, we have found that new interlayer interactions (As1-As2 and As1-S1) are formed at the expense of the intralayer interaction between As2 and S1; the Mulliken bond-overlap populations for the As1-As2 and As1-S1 bonds in model 2 were calculated to be 0.380 and 0.384, respectively. That is, both As2 and S1 interact covalently with a pnictogen atom (As1) in the neighboring layer. Consequently, a fivefold-coordinated As unit centered on the As1 atom is created, having four As-S bonds and one As-As (As1-As2) bond, resulting in a trigonal bipyramidal structure, in which the two equivalent sulfur atoms (S1 and S7) are at somewhat greater distances (~2.4 Å) from the central As1 atom than the other sulfur atoms (~2.2 Å). Such a fivefold-coordinated site in model 2 is basically identical with that reported in our previous paper.[29] This strongly suggests that the structural transformation from threefold- to fivefold-coordinated As is not an artifact of the calculations using small clusters, but is likely to occur in actual systems after photoinduced intralayer bond breaking.

It should be noted, however, that the situation of models 3 and 4, in which the As3-S1 and As4-S2 bonds, respectively, are intentionally elongated prior to its rupture, is entirely different from that of model 2. As shown in Fig. 1(c), atom As3 (As4) in model 3 (model 4) appears to interact covalently with the As atom in a neighboring layer, forming a fourfold-coordinated As unit centered on the As1 (As3) atom. On the other hand, atom S1 (S2) in model 3 (model 4) does not form any additional bond with nearby As and S atoms; that is, atom S1 (S2) in model 3 (model 4) can be described as a nonbridging sulfur atom. A weakening of the intralayer As3-S1 and As4-S2 bonds in models 3 and 4, respectively, hence creates only one interlayer As-As bond (As1-As3 and As3-As4 in models 3 and 4, respectively). It is also worth mentioning that the total energies of models 3 and 4 are only slightly lower than that of another metastable form of the cluster, namely, model 2; the energy difference between models 2 and 3 is 0.006 eV and that between models 2 and 4 is 0.137 eV. Thus, as far as the calculated total energies are concerned, we cannot decide which configuration (model 2, 3, or 4) is more energetically favorable as a metastable defect structure.

B. Charge distribution

Table II shows calculated Mulliken atomic charges q for the principal As and S atoms in the present model clusters. We see from Table II that the As and S atoms in model 1 can be regarded in principle as being neutrally charged in terms of a Mulliken population analysis. In model 2, however, As2 and S1 are positively ($q_{As2}=+0.203$) and negatively ($q_{S1}=-0.214$) charged, respectively, implying that the intralayer bond breaking is accompanied by a charge separation to form positively and negatively charged defects. Note also that S7 in model 2 has a considerable negative charge ($q_{S7}=-0.342$) as compared with the corresponding atom in model 1 ($q_{S7}=-0.126$), indicating delocalization of the negative charge over the two equivalent S atoms in the fivefold-coordinated As unit. In model 3, such a charge separation is more obvious in the atomic charges of As3 and S1 ($q_{As3}=+0.329$, $q_{S1}=-0.580$). The same tendency can also be seen in the atomic charges of As4 and S2 ($q_{As4}=+0.238$, $q_{S2}=-0.523$). We hence suggest that photoin-

TABLE II. Mulliken atomic charges calculated for the model clusters.

	Model 1	Model 2	Model 3	Model 4
As1	0.006	0.032	0.032	0.068
As2	0.030	0.203	0.169	−0.038
As3	0.048	0.037	0.329	0.065
As4	0.026	0.046	0.197	0.238
As5	0.043	0.009	0.020	0.095
As6	0.127	0.112	0.093	0.170
As7	0.077	0.128	0.124	0.121
S1	−0.068	−0.214	−0.580	0.055
S2	−0.055	0.004	−0.017	−0.523
S3	−0.060	0.050	−0.076	−0.207
S4	−0.080	−0.066	−0.071	−0.008
S5	−0.085	−0.073	−0.218	−0.035
S6	−0.116	−0.009	0.003	−0.161
S7	−0.126	−0.342	−0.060	−0.225

duced changes in the structure and optical properties of a-As_2S_3 can be interpreted in terms of the charge separation caused by intralayer bond breaking and subsequent atomic rearrangements.

C. Molecular-orbital structure

It is interesting to investigate how the atomic reconfigurations shown in Fig. 1 affect the orbital energies of the respective clusters. Figure 2 shows an energy diagram for the highest occupied molecular orbital (HOMO) of the present model clusters. Analyzing the linear weighting coefficients of the atomic orbitals, we have found that the HOMO of model 1 is characterized mostly by nonbonding S $3p$-type orbitals and As $4s$- and $4p$-type orbitals [see also Fig. 3(a)]. These nonbonding ns- and/or np-type orbitals of S and As atoms contribute to the HOMO levels of models 2, 3, and 4 as well. In model 2, however, the As1-As2 bonding orbital derived from the fivefold-coordinated As1 atom also makes a significant contribution to the HOMO level [see also Fig. 3(b)]. Accordingly, the HOMO level of model 2 is raised by ~0.3 eV as compared with the case of model 1. Thus it is reasonable to expect that the absorption edge shifts to lower energies as a result of the photoinduced formation of fivefold-coordinated As units, each having one As-As bond. One also notices from Fig. 2 that the HOMO level is further raised by ~1 eV as we go from model 2 to models 3 and 4.

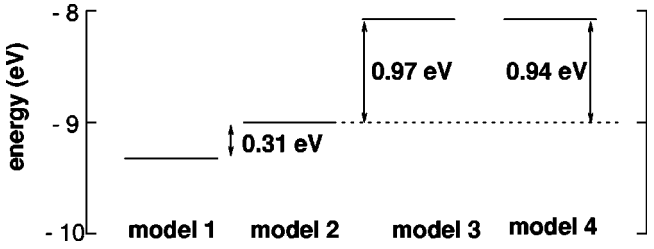

FIG. 2. Molecular energy diagram showing the HOMO of the respective model clusters calculated at the HF/6-31G(d) level.

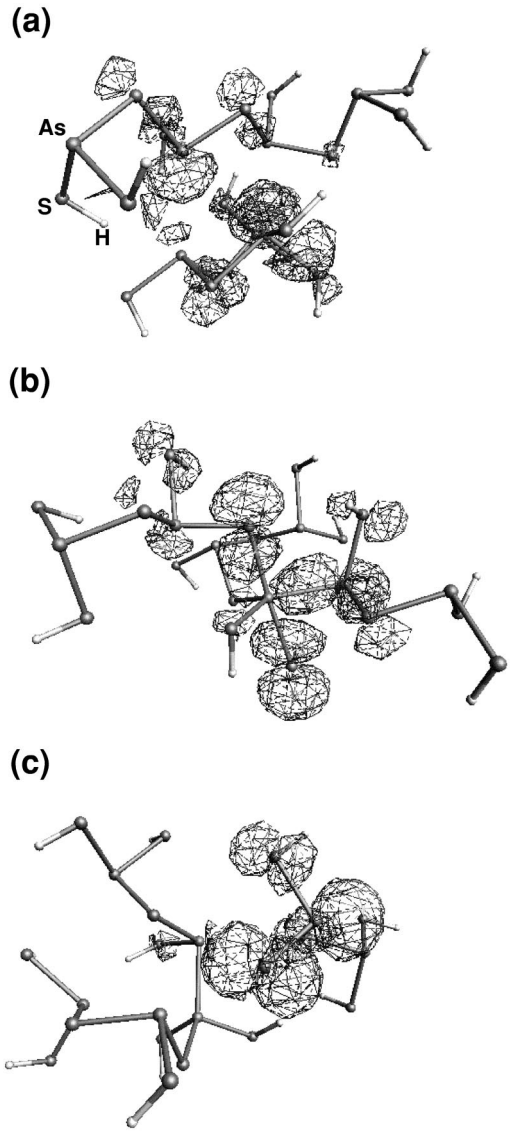

FIG. 3. Three-dimensional representations of the HOMO of the model clusters calculated at the HF/6-31G(d) level: (a) model 1, (b) model 2, and (c) model 3.

Since the HOMO level of model 3 (model 4) is composed mainly of the nonbonding $3p$-type orbitals of S1 (S2) [see also Fig. 3(c)], it is most likely that the nonbridging S atom is responsible especially for the lower-energy component of the photoinduced optical absorption.

D. Electron excitation energy

Table III shows the calculated singlet-to-singlet excitation energies of the present model clusters obtained using the TD-DFRT method. In harmony with the changes in the HOMO levels, the calculated first excitation (S_0-S_1) energy decreases in the order model 1 (3.54 eV), model 2 (2.49 eV), and models 3 and 4 (1.78 and 1.60 eV, respectively). Indeed, we have confirmed that electron excitation from the HOMO level contributes mostly to each S_0-S_1 excitation, indicating

TABLE III. First (S_0-S_1), second (S_0-S_2), and third (S_0-S_3) singlet-to-singlet excitation energies (E, in eV) and oscillator strengths (f) calculated for the model clusters.

	Model 1		Model 2		Model 3		Model 4	
	E	f	E	f	E	f	E	f
S_0-S_1	3.54	0.0036	2.49	0.0225	1.78	0.0008	1.60	0.0006
S_0-S_2	3.69	0.0133	2.58	0.0029	2.09	0.0004	1.98	0.0015
S_0-S_3	3.74	0.0023	2.72	0.0559	2.42	0.0042	2.31	0.0118

that these changes in the excitation energy result from the atomic rearrangements that can affect considerably the corresponding HOMO levels.

IV. DISCUSSION

A. Metastability of the defect structures

We have shown that there exist at least two types of metastable defects in the As_2S_3 network. One (model 2) has a fivefold-coordinated As unit, and the other (models 3 and 4) consists of a fourfold-coordinated As atom and a nonbridging S atom. It should also be noted that both of the metastable defects have an As-As bond, suggesting an important role of interlayer As-As linkages in the process of photostructural changes.

As mentioned above, the total energy of model 2 is almost identical with that of models 3 and 4. However, the formation of the coordination defect shown in model 2 requires much more complicated atomic rearrangements than the formation of the defect shown in model 3 (or model 4). Stated in another way, the metastable defect configuration in model 2 should be more stable against reformation of the original intralayer As-S/bond as compared with the case of the metastable defect shown in model 3 (or model 4), as shown in Fig. 4. Thus the photoinduced defect structure in model 2 might be more stable against thermal annealing than that in model 3 (or model 4). Furthermore, the calculated excitation energies shown in Table III imply that the metastable defects shown in models 2 and 3 (or model 4) contribute, respectively, to the higher- and lower-energy components of the photoinduced shift of the absorption edge.

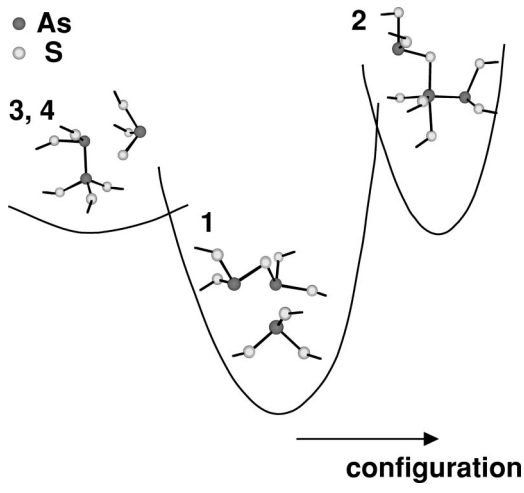

FIG. 4. Possible configurational-coordinate potential-energy diagram illustrating schematically the relative energies of the ground-state (model 1) and metastable-state (models 2, 3, and 4) configurations in a-As_2S_3. The energy barrier for the structural relaxation from 2 to 1 is expected to be higher than that from 3 (or 4) to 1.

The present calculated results can provide a reasonable explanation for the annealing behavior of the photoinduced optical absorption spectra of a-As_2S_3. It has been reported that the spectrum caused by irradiation at low temperatures ($\sim$10 to $\sim$30 K) cannot simply be characterized by a parallel shift of the absorption edge, but shows an additional midgap absorption.[37,38] The midgap absorption below $\sim$2 eV disappears with thermal annealing at 150 K; however, the edge remains shifted to a lower energy by $\sim$0.2 eV, showing a spectrum similar to that induced by illumination at room temperature. This indicates that there can be at least two different components that are responsible for the photoinduced absorption.[1,37] We consider that the metastable defect shown in model 3 (or model 4) is mainly responsible for the midgap absorption below $\sim$2 eV induced by irradiation at low temperatures. As mentioned earlier, the defect structure in model 3 (or model 4) is expected to be reformed easily and it gives rise to a lower excitation energy than that of model 2. Thus it is likely that the defect consisting of the nonbridging S and fourfold-coordinated As in model 3 (or model 4) plays a role in the low-temperature or the low-energy component of the photoinduced absorption edge. On the other hand, the defect structure seen in model 2 can be responsible for the high-temperature or the high-energy component of the photoinduced shift of the absorption edge, explaining the photodarkening induced by irradiation at room temperature.

B. Mechanisms of electron-phonon coupling

We see from Table II that the present atomic rearrangements generating the metastable defects shown in models 2, 3, and 4 are accompanied by appreciable charge separation, suggesting a mechanism of strong electron-phonon coupling in the photoinduced process. A mechanism of electron-phonon coupling was originally proposed by Street[19] to account for the reversible photostructural changes in chalcogenide glasses. He proposed that an optically created exciton could thermally transform to a conjugate pair of charged (diamagnetic) dangling-bond defect states: that is,

$$\text{exciton} \rightarrow D^+ + D^-$$

where D^+ and D^- are positively and negatively charged defects, respectively. The present calculations basically support the above mechanism, in which nonradiative recombination proceeds through the creation of these metastable charged defects. Although the present calculations demonstrate that the charge on the defect site is not solely localized on one particular atom, but is delocalized over its first- and second-coordination shells (see Table II), we consider that the photocreation of a charged defect pair is a useful model to interpret qualitatively the photostructural effects of a-As_2S_3.

The present calculations further elucidate that the transient bond rearrangements obtained are not unique, but can lead to at least two different types of charged defect configurations. According to the D^+,D^- nomenclature, the defect configuration in models 3 and 4 can be described as As_4^+,S_1^- (involving atoms As1 and S1 in model 3 and atoms As3 and S2 in model 4), where the superscript refers to the charge state and the subscript refers to the coordination of the dangling-bond defect. Although such an As_4^+,S_1^- pair has been supposed to exist as a metastable defect in a-As_2S_3, this is the first theoretical work to our knowledge that can show the microscopic structure of the charged defect pair. We should note, however, that the positive charge is not located mainly on the fourfold-coordinated As atom in the defect (As1 in model 3 and As3 in model 4), but on its adjacent As atom (As3 in model 3 and As4 in model 4), forming a homopolar As-As bond and also on next-nearest-neighbor As atoms (e.g., As4 in model 3 and As6 in model 4: see Table II), indicating that this charged defect should not be described simply as As_4^+,S_1^- in the strict sense.

As for the charged defect in model 2, there is no apparent broken bond in the defect site, and one of the As atoms in the defect (As1) is fivefold coordinated. Similar to the case of the charged defect in model 3, the positive charge is not located on the overcoordinated As atom (As1); rather, the positive charge is located on the other side of the homopolar As-As bond: namely, on As2. Even in such a case, the idea of charge separation may still hold since we see a spatial separation (3.2–3.5 Å) between the charged As (As2) and S (S1 and S7) atoms in the defect site.

V. CONCLUSIONS

In this work, two types of metastable photoinduced defect structures have been shown to exist on the basis of quantum-chemical calculations of clusters of atoms modeling the local structure of a-As_2S_3. One is a fivefold-coordinated As unit, as has been proposed in our recent paper.[29] The other comprises a fourfold-coordinated As unit and a nonbridging S atom. It has been found that the former metastable defect yields a higher excitation energy than the latter one. It is hence quite likely that the fivefold-coordinated As unit is mainly responsible for the high-energy component of the observed photoinduced shift of the absorption edge. On the other hand, the metastable defect consisting of a fourfold-coordinated As unit and a nonbridging S atom will contribute to the low-energy component (or a midgap absorption) which disappears with low-temperature annealing. It should be stressed that these two metastable defects originate from interlayer bond reconstruction to form As-As homopolar bonds, suggesting a vital role of interlayer defect-transformation processes in causing photoinduced metastability and photodarkening.

ACKNOWLEDGMENTS

We would like to thank Ke. Tanaka, K. Shimakawa, and A. Ganjoo for useful discussions.

*Present address: Department of Chemistry, Faculty of Science, Kobe University, Nada-ku, Kobe 657-8501, Japan. Electronic address: uchino@kobe-u.ac.jp

[1] K. Shimakawa, A. Kolobov, and S. R. Elliott, Adv. Phys. **44**, 475 (1995).
[2] H. Fritzsche, in *Insulating and Semiconducting Glasses*, edited by P. Boolchand (World Scientific, Singapore, 2000).
[3] K. Tanaka, Appl. Phys. Lett. **26**, 243 (1975).
[4] H. Hisakuni and Ke. Tanaka, Appl. Phys. Lett. **65**, 2925 (1994).
[5] Ke. Tanaka, Phys. Rev. B **57**, 5163 (1998).
[6] L. F. Gladden, S. R. Elliott, and G. N. Greaves, J. Non-Cryst. Solids **106**, 189 (1988).
[7] S. R. Elliott and A. V. Kolobov, Philos. Mag. B **61**, 853 (1990).
[8] C. Y. Yang, M. A. Paesler, and D. E. Sayers, Phys. Rev. B **36**, 9160 (1987).
[9] G. Pfeiffer, C. J. Brabec, S. R. Jefferys, and M. A. Paesler, Phys. Rev. B **39**, 12 861 (1989).
[10] J. M. Lee, M. A. Paesler, D. E. Sayers, and A. Fontaine, J. Non-Cryst. Solids **123**, 295 (1990).
[11] S. G. Bishop, U. Strom, and P. C. Taylor, Phys. Rev. B **15**, 2278 (1977).
[12] J. A. Freitas, Jr., U. Strom, and S. G. Bishop, Phys. Rev. B **35**, 7780 (1987).
[13] K. Shimakawa, S. Inami, and S. R. Elliott, Phys. Rev. B **42**, 11 857 (1990).
[14] A. Ganjoo, K. Shimakawa, N. Yoshida, T. Ohono, A. V. Kolobov, and Y. Ikeda, Phys. Rev. B **59**, 14 856 (1999).
[15] Ke. Tanaka, Solid State Commun. **28**, 541 (1978).
[16] P. Krecmer, A. M. Moulin, R. J. Stephenson, T. Rayment, M. E. Welland, and S. R. Elliott, Science **277**, 1799 (1997).
[17] Ke. Tanaka, Solid State Commun. **34**, 201 (1980).
[18] S. R. Elliott, J. Non-Cryst. Solids **81**, 71 (1986).
[19] R. A. Street, Solid State Commun. **24**, 363 (1977).
[20] H. Fritzsche, Solid State Commun. **99**, 153 (1996).
[21] S. R. Elliott and K. Shimakawa, Phys. Rev. B **42**, 9766 (1990).
[22] M. Popescu, J. Non-Cryst. Solids **90**, 533 (1987).
[23] For a recent review, see M. Popescu, *Non-Crystalline Chalcogenides* (Kluwer, Dordrecht, 2000).
[24] T. Uchino, Y. Kitagawa, and T. Yoko, Phys. Rev. B **61**, 234 (2000).
[25] T. Uchino, M. Takahashi, and T. Yoko, Phys. Rev. B **62**, 2983 (2000); Phys. Rev. Lett. **86**, 1777 (2001); **86**, 4560 (2001); **86**, 5522 (2001).
[26] G. Pacchioni and R. Ferrario, Phys. Rev. B **58**, 6090 (1998).
[27] B. L. Zhang and K. Raghavachari, Phys. Rev. B **55**, R15 993 (1997).
[28] K. Raghavachari and G. Pacchioni, J. Chem. Phys. **114**, 4657 (2001).
[29] T. Uchino, D. C. Clary, and S. R. Elliott, Phys. Rev. Lett. **85**, 3305 (2000).
[30] A. H. Edwards, W. B. Fowler, and J. Robertson, in *Structure and Imperfections in Amorphous and Crystalline Silicon Dioxide*, edited by R. A. B. Devine, J.-P. Duraud, and E. Dooryhée (Wiley, Chichester, 2000), p. 253, and references therein.

[31] P. C. Hariharan and J. A. Pople, Mol. Phys. **27**, 209 (1974), and references therein. For As atoms, we used the $(14s11p5d)$ basis set reported in T. H. Dunning, Jr., J. Chem. Phys. **66**, 1382 (1977).

[32] M. J. Frisch, G. W. Trucks, H. B. Schlegel, G. E. Scuseria, M. A. Robb, J. R. Cheeseman, V. G. Zakrzewski, J. A. Montgomery, R. E. Stratmann, J. C. Burant, S. Dapprich, J. M. Millam, A. D. Daniels, K. N. Kudin, M. C. Strain, O. Farkas, J. Tomasi, V. Barone, M. Cossi, R. Cammi, B. Mennucci, C. Pomelli, C. Adamo, S. Clifford, J. Ochterski, G. A. Petersson, P. Y. Ayala, Q. Cui, K. Morokuma, D. K. Malick, A. D. Rabuck, K. Raghavachari, J. B. Foresman, J. Cioslowski, J. V. Ortiz, B. B. Stefanov, G. Liu, A. Liashenko, P. Piskorz, I. Komaromi, R. Gomperts, R. L. Martin, D. J. Fox, T. Keith, M. A. Al-Laham, C. Y. Peng, A. Nanayakkara, C. Gonzalez, M. Challacombe, P. M. W. Gill, B. G. Johnson, W. Chen, M. W. Wong, J. L. Andres, M. Head-Gordon, E. S. Replogle, and J. A. Pople, *Gaussian 98, Revision A7* (Gaussian Inc., Pittsburgh, 1998).

[33] R. S. Mulliken, J. Chem. Phys. **23**, 1833 (1955).

[34] M. E. Casida, C. Jamorski, K. C. Casida, and D. R. Salahub, J. Chem. Phys. **108**, 4439 (1998).

[35] R. E. Stratmann, G. E. Scuseria, and M. J. Frisch, J. Chem. Phys. **109**, 8218 (1998).

[36] A. D. Becke, J. Chem. Phys. **98**, 5648 (1993).

[37] K. Tanaka, in *Structure and Excitation of Amorphous Solids*, edited by G. Lucovsky, and F. L. Galeener, AIP Conf. Proc. No. 31 (AIP, New York, 1976), p. 148.

[38] D. K. Biegelsen and R. A. Street, Phys. Rev. Lett. **44**, 803 (1980).